CONF-791069--3

MASTER

# OPTIMAL DESIGN
# OF
# COMPRESSED AIR ENERGY STORAGE SYSTEMS

by

F.W. Ahrens, A. Sharma and K.M. Ragsdell





Prepared for

6th Annual UMR-DNR Conference and Exposition on Energy

Rolla, Missouri

October 16-18, 1979



U of C-AUA-USDOE

**ARGONNE NATIONAL LABORATORY, ARGONNE, ILLINOIS**

**Operated under Contract W-31-109-Eng-38 for the**

**U. S. DEPARTMENT OF ENERGY**

## DISCLAIMER

6th Annual UMR-DNR Conference and Exposition on Energy
University of Missouri - Rolla
October 16-18, 1979

# Optimal Design of Compressed Air Energy Storage Systems

by

F. W. Ahrens, Argonne Nat'l Lab, Argonne, IL
A. Sharma, UICC, Chicago, IL
K. M. Ragsdell, Purdue Univ., W. Lafayette, IN

## Abstract

Compressed air energy storage (CAES) power systems are currently being considered by various electric utilities for load-leveling applications. In this paper we develop models of CAES systems which employ natural underground aquifer formations, and present an optimal design methodology which demonstrates their economic viability. This approach is based upon a decomposition of the CAES plant and utility grid system into three partially-decoupled subsystems. Numerical results are given for a plant employing the Media, Illinois Galesville aquifer formation.

## 1. INTRODUCTION

Compressed air energy storage is one of the technologies that is currently available to electric utilities to supply peak power using stored energy previously generated during periods of excess capacity. The use of energy storage systems can be economically advantageous to utilities, since they improve the utilization of high efficiency base plants, which have high capital but relatively low operating costs. Another major benefit of using energy storage systems is the reduction of premium fuel required in generating peak power. At present, the only commonly used energy storage technique is above ground pumped hydro, but the world's first CAES plant has recently been built in West Germany[1]. A demonstration program for CAES and underground pumped hydro is underway in the U.S.A., co-sponsored by the Department of Energy and the Electric Power Research Institute. Although CAES already appears to be a technically and economically viable option[2-5], it will surely come into use more rapidly if the economic incentives can be improved. The material in this paper discussing the optimal design of CAES systems, is relevant to this goal.

Consider the CAES power plant given in Figure 1, which is based on a split Brayton cycle, and composed of four equipment groups: a reversible motor/generator, air compression equipment, an air storage reservoir (with associated piping), and power extraction equipment. The use of the couplings on the motor/generator allows either electrical power from the utility grid to be used in compressing air or power to be generated, using the stored compressed air and some premium fuel (about one-third to one-half as much as consumed in conventional combustion turbine peaking units). The CAES system configuration shown in Fig.1 is typical, but many variations in equipment are possible[5-7]. In terms of its interaction with the other equipment groups, the turbine system can be characterized by its design inlet pressure ($p_{tt}$) and its mass flow rate per unit power output ($\dot{m}'$). The latter depends on the turbine inlet temperatures (premium fuel consumption), and equipment arrangement and design. Details of these relationships are discussed elsewhere[7-9]. Because of the requirements for storing large amounts of high pressure compressed air (e.g. $10^7$-$10^9$ ft$^3$ at 50 atm for a typical 200 MW plant), it is known that underground air reservoirs are an economic necessity. The reservoir can be either a cavern (in hard rock or in a salt dome) or a porous rock layer (most commonly an aquifer), such as the edge water aquifer shown in Figure 2. The choice of which type of reservoir should be used depends, of course, on the geological conditions of the region in which the plant is to be sited.

The storage reservoir design requirements (capacity, pressure level, piping design, etc.) are interdependent with the selection (performance characteristics and operating conditions) of the above-ground compression and power generation equipment, and the desired power output and operating cycle of the CAES plant. In turn, the decision on the power level and duty cycle is impacted by the economic and technical characteristics of the utility grid, by the cost of premium fuel, etc. Furthermore, we expect that the design construction and operation of a CAES plant would involve the investment of large amounts of capital. Many technical and economic tradeoffs must be considered in specifying a CAES plant design. The scale of technology involved in a CAES plant is of the same order of magnitude as that in any conventional power plant. Therefore, the only practical way of designing such a large system, without the benefit of previously developed standards, is to automate the design procedure. Any attempt at manual design would require a tremendous input of manpower and it would be difficult to guarantee a feasible much less an optimal design. Although CAES plant design studies have been performed[4,5,10,11], and these have included some attempts to optimize certain components of the system, detailed CAES system economic optimizations have not been reported. The objective of this paper is to present a comprehensive optimum design approach.

We shall see in the following discussion that the system model is complex, and leads us to employ a decoupling or decomposition technique in order to more efficiently seek optimal designs. The optimal design approach presented is most easily justified as an efficient and accurate method of site comparison and selection. There are other advantages to the approach, which will we trust be obvious from the results of our study.

## 2. CAES SYSTEM MODEL

As we have seen in Figure 1, broadly speaking, a CAES power system is composed of the following: the air compression train (compressors, intercoolers, aftercoolers); compressed air piping; air storage reservoir (any type); power generation train (turbines, combustors, recuperators); reversible motor/generator and the utility grid. Although the utility grid is not physically part of the CAES plant, the interaction should be considered, since the cost of base load power and the utility load cycle may have a strong influence on design cost of the CAES facility. Correspondingly, the CAES costs will influence the cost of power sold by the utility.

### 2.1 *Decomposition Strategy*

We find it convenient, if not essential, to decompose the system into three group or subsystems as seen in Figure 3. Subsystem 1 contains the air storage reservoir, air compression train, and main piping and air distribution system. Subsystem 2 contains the power generation train, and subsystem 3 contains the motor/generator and the utility grid. With the subsystems formed in this way, it is possible to choose coupling and internal variables so that the subsystems can be designed with a degree of independence from the other subsystems. The exact dependence is contained in the coupling variable relationships. For instance, in our work we assume that subsystem 3 (the utility grid) affects the rest of the system through a variable, $U_L$, the utility load cycle as shown in Figure 4. This single variable could, of course, represent many variables in the utility load cycle, but this is not pursued here since our interest is primarily with subsystems 2 and 3. The coupling influence should be clear. Finally, we suggest that the direct interactions (or coupling) between subsystems 1 and 2 are dependent on only two variables; namely, the inlet pressure to the power generation train ($p_{ti}$), and the specific air mass flow rate ($\dot{m}'$). As the figure suggests, there is the indirect influence of the utility load cycle as well. In this work we eliminate this effect by choosing the load cycle.

The criterion for optimal design is chosen to be the total normalized cost (C) of the system (i.e., cost per unit of electricity generated by the CAES power plant). This total cost is the sum of the individual costs which normally include fuel cost, maintenance, charge rate on capital, etc. The costs have to be minimized subject to various performance and technical constraints. The implication for CAES plant design is that, for a given utility load cycle, an optimization of subsystem 1 would provide the minimum subsystem operating cost ($C_1^*$) and values for the corresponding subsystem design variables. as a function of the coupling variables, $p_{ti}$ and $\dot{m}'$. Similar optimization for subsystem 2 would yield $C_2^*$ (the minimum operating cost of subsystem 2) and its optimum design, as a function of the coupling variables only. Finally, the sum of $C_1^*$ and $C_2^*$ can be minimized to determine the optimum values of the coupling variables, the minimum plant cost ($C^*$) and the optimal plant design. The process can obviously be expanded (in principle) to include variations in the utility load cycle and consideration of the resulting economic benefits or penalties to the utility. The remainder of this paper is confined to the design of a particular variety of subsystem 1 (one with an aquifer reservoir), to the design of subsystem 2, and to the synthesis of an optimal design for the CAES plant, using the subsystem 1 and 2 results.

### 2.2 Subsystem 1: Storage

An aquifer (originally water-filled) is an underground porous medium, which for storage should have the shape of an inverted saucer (see Figure 5) to prevent migration of the compressed air. The air bubble is formed by displacing the innate water; the compressed air is contained between the air tight caprock and a bottom layer of water. The operational constraints for utilizing such a formation are discussed by Ahluwalia[12]. The compressor train included in this subsystem follows the recommendations of United Technologies Research Center[13]. To illustrate the procedure, a simplified piping and distribution system was adopted. The following discussion briefly describes the technical modeling of subsystem 1. A detailed discussion of the model employed is given by Ahluwalia[12], where an explanation of all the cost functions is also included. Here, we focus on the formulation of the optimal design problem.

In the optimization of subsystem 1, the objective is to determine the combination of internal design variables which minimizes the subsystem operating cost, for given values of the coupling variables, $p_{ti}$, $\dot{m}'$ and $U_L$. The set of design variables can be classified into two subsets. The first subset includes variables which are restricted to take a limited number of discrete values. Engineering considerations require that the main piping diameter, the type of low pressure compressor, and the reservoir well bore diameters be restricted to discrete, economically available designs. As the number of alternates is limited, a simple method of incorporating these discrete variables in the optimization is an exhaustive search in all discrete dimensions. Therefore, the following formulation assumes that the parameters resulting from the selection of a main piping system, low pressure compressor, and the well bore diameter are temporary "constants". The final step in optimization would be a search for minima in the parametric "constant" space. The remaining internal variables of subsystem 1 are treated as continuous variables to be optimized, in a bound and constrained space. These variables are four geometric parameters of the reservoir design; $N_W$, H, $A_{act}$, and d, illustrated in Figure 5; and the energy storage process variables $t_{cb_i}$ and $t_{ce_i}$. The variables $t_{cb_i}$ represent the times during the weekly cycle when energy storage processes begin and $t_{ce_i}$ are the ending times of these processes. The storage (charging) time variables are shown, for a typical cycle, in Figure 4. The operating cost, to be minimized, can be written as

$$C_1(N_W,H,A_{act},d,t_{cb_i},t_{ce_i}) = K_1(U_L)C_T + K_2(U_L)P_{C_i}\sum_i(t_{ce_i}-t_{cb_i}). \quad (2.1)$$

In the equation above, $K_1$ and $K_2$ are functions of the coupling variable $U_L$ but are treated as constants for the purpose of optimization. Similar notation is used to represent functions of other coupling variables and functions of the three discrete internal variables. Absolute constants appear in the following without any functional dependence shown. However, for the purpose of the optimization problem statement, all K's can be treated as constants. The first term in equation (2.1) represents the operating cost due to the annual charge rate on capital, $C_T$, of subsystem 1, where $C_T$ is the sum of capital costs of the various components:

$$C_T(N_W,H,A_{act},d,t_{cb_i},t_{ce_i}) = WC + LC + BC + CC + K_3(\text{piping}). \quad (2.2)$$

$K_3$(piping) is the capital cost of the main piping and distribution system which depends upon the piping design selected. The capital cost of wells is: (2.3)

$$WC(N_W,H,A_{act}) = N_W[K_{W_1} + K_{W_2}\{H - F(A_{act})\}],$$

with constants $K_{W_1}$, $K_{W_2}$, and $F(A_{act})$, a known function of $A_{act}$ determined from reservoir geometry. The term within curly brackets in equation (2.3) is the depth to which wells have to be bored. The second term in equation (2.2) is the cost of purchasing the land over the proposed reservoir;

$$LC(d) = K_4\ A(d), \quad (2.4)$$

where A(d) is the land area over the air reservoir, a known geometric function of d.

In this simplified model, the capital cost of initially displacing water from the aquifer, or bubble development, is calculated in terms of energy required to compress the volume of air in the bubble, which is a function of d. Finally, the capital cost of the compressor train is expressed as:

$$CC(N_W,H,A_{act},d,t_{cb_i},t_{ce_i}) \quad (2.5)$$
$$= K_{c\ell_1} + K_{c\ell_2}\dot{M}_C + K_{cb_1}\left[\dot{M}_C\left\{\frac{P_C}{K_{c\ell_3}} - 1\right\}\right]^{K_{cb_2}}$$

Here, $K_{c\ell_1}$, $K_{c\ell_2}$, and $K_{c\ell_3}$ are parametric constants determined by the choice of compressor train design. $\dot{M}_C$ is the air mass flow rate during the storage processes, chosen to be the same during all storage processes due to compressor performance considerations. $K_M$ is another "constant" determined by the coupling variables $U_L$ and $\dot{m}'$. the remaining unknown term in equation (2.5) is $P_C$, the discharge pressure required of the compressor train. This pressure can be calculated using the pressure drop models given by Sharma[14]. The second term in equation (2.1) is the subsystem operating cost incurred due to compressor power consumption, $P_C$, which is given by:

$$P_C(N_W,H,A_{act},d,t_{cb_i},t_{ce_i}) \quad (2.6)$$
$$= [K_{P_1} + K_{P_2}P_C + K_{P_3}P_C^2 + K_{P_4}P_C^3]\dot{M}_C.$$

The functional dependences of the objective function are summarized in the subproblem graph of Figure 6.

Engineering intuition, aquifer geology and geometry, and the utility load cycle suggest bounds and functional constraints on the design variables. These have been completely developed and explained by Ahrens[15] and will not be repeated here. In summary, we place bounds on the storage process times as suggested in Figure 4, and upper and lower limits on the four physical variables, $N_W$, H, $A_{act}$, and d as defined in Figure 5. Functional constraints are imposed which require that all storage processes end after they begin, that the wells be placed close enough to ensure full utilization of reservoir volume, that the well bores not physically interfere one with another, that the "bubble" be no larger than the land purchased, that the wells not be drilled to a depth that would cause "coning", that the required compressor power be less than that which the utility is willing and/or able to supply at anytime, and finally, that the pressure requirement of subsystem 2 is met at all times by subsystem 1. In summary, there are 16 design variables with 32 bounds, and 12 constraints, 4 of which are nonlinear.

## 2.2 Subsystem 2: Generation

Subsystem 2 of the CAES system is composed of the high and low pressure turbines, their combustors and the recuperator, as indicated in Figure 1. It is also considered to include the balance-of-plant (assumed not to be variable). The most interesting design tradeoffs for this subsystem are: (a) larger, more effective recuperator vs. greater premium fuel consumption in the combustors, for preheating the air entering the turbines, and (b) advanced, high inlet temperature turbines, having high cost but high performance vs. conventional, lower temperature, lower cost turbines. An additional tradeoff, of secondary importance, is the pressure ratio split between the high-pressure turbine and the low-pressure turbine.

The performance model for subsystem 2 is based on a thermodynamic analysis (i.e., mass and energy balance equations) of the components. The detailed equations are given by Kim[16,17]. It should be mentioned, however, that the model includes the effect that as the turbine inlet temperatures are increased above a certain threshold value (taken to be 1600°F), it is necessary to use an increasing fraction of the compressed air from storage to provide cooling for the turbine blades and other turbine components.

For the purpose of calculating the subsystem 2 performance, the coupling variables, $p_{ti}$ (the subsystem inlet pressure) and $\dot{m}'$ (the specific turbine system air flow rate, $lb_m$/kWh), and $P_{gen}$, the total power output from the two turbines, are regarded as inputs. Because of this, it is not possible to independently specify both turbine inlet temperatures, $T_3$ and $T_5$, if fixed, state-of-the-art, turbine efficiencies are assumed. In the present model, $T_5$ (low-pressure turbine inlet temperature) was considered as a design variable and $T_3$, along with several intermediate variables, was subsequently determined during the iterative solution of the model equations. The other design variables of subsystem 2 are the recuperator effectiveness, $\varepsilon$, and the low-pressure turbine pressure ratio, r $(=p_5/p_6)$. The variable $r_p$ was considered to be discrete. Its two values (11 and 16) correspond to the current practise of turbomachinery manufacturers. With specified values of the design variables, other operating conditions and performance characteristics are predicted from the solution of the model equations. Of particular note is the specific heat rate, $\dot{Q}'$ (Btu/kWh), which is proportional to the rate of premium fuel consumption of the CAES plant.

In the optimization of subsystem 2, the objective is to find the combination of internal design variables which minimizes the subsystem operating cost, for given values of the coupling variables. During a particular optimization process, the coupling variables, $p_{ti}$ and $\dot{m}'$, and $U_L$, are fixed, so will be omitted from the functional relationships which follow. The discrete variable $r_p$ is also omitted, since an optimization is performed separately for each of its values. The operating cost to be minimized can be written as:

$$C \quad (T_5,\varepsilon) = K_1(U_L)C_{cap}' + K_F\dot{Q}' + K_{om} \qquad (2.7)$$

The first term represents the operating cost due to the annual charge rate on the capital, $C_{cap}'$, of subsystem 2, where $C_{cap}$ is the sum of capital costs:

$$C_{cap} \; (T_5,\varepsilon) = C_{LGT} + C_{HGT} + C_R + C_{BAL} \qquad (2.8)$$

According to expression (2.8), the capital cost is the sum of the cost of the low pressure turbine (including the increase expense of cooling air for high operating temperature), $C_{LGT}$; the cost of the high pressure turbine, $C_{HGT}$; the cost of the recuperator, $C_R$; and the cost of the balance of plant, $C_{BAL}$. We employ the cost relationship given by Kim[17,18] and assume a yearly operating time of 2500 hours at full power. The second term in equation (2.7) is the cost of the premium fuel used in the combustors. $K_F$ is taken as \$2.50/$10^6$ Btu. The heat rate, $\dot{Q}'$, is dependent on $T_3(T_5,\varepsilon)$ and $T_5$. The final term in equation (2.7) is the operating and maintenance cost of the plant. It is considered to have a constant value, 2 mills/kWh. Finally, we place upper and lower bounds on the three design variables; $\varepsilon$, the recuperator effectiveness; $T_3$ and $T_5$, the turbine inlet temperatures.

## 3. OPTIMIZATION METHODS

Modern optimization theory was born of the logistical needs of World War II and the pioneering work of George Dantzig[19]. In the early years, work in this country addressed problems where all functions involved were linear in the design variables. In this section we consider the more practical, yet difficult problem where all functions are nonlinear. The methods which follow are modern methods, which are useful for today's energy management problems. All of the methods assume the presence of a modern third-generation digital computer. In particular we consider algorithms for the nonlinear programming problem:

$$\text{minimize:} \quad f(x),\; x=[x_1,x_2,x_3\ldots,x_N] \in R^N \qquad (3.1)$$

$$\text{subject to:} \quad g_j(x)\geq 0 \;\; j=1,2,3,\ldots,J \qquad (3.2)$$

$$h_k(x)\equiv 0 \;\; k=1,2,3,\ldots,K \qquad (3.3)$$

where f(x) is the objective, a scalar function of the design variables x, and $g_j(x)$, and $h_k(x)$ are the inequality and equality constraint functions, respectively. These functions $f(x)$, $g_j(x)$, $h_k(x)$ are assumed to be nonlinear but not necessarily algebraic; that is, they need only be calculable functions of x. The inequality constraints are often called regional constraints, because they disallow complete regions of the design space. The equality constraints define exact relationships that must exist between the design variables and are therefore more difficult to handle for most algorithms. The methods to be considered generate a sequence of points $x^{(m)}$, m=1,2,3,...,M, where $x^{(M)}$ is an estimate of the solution $x^*$. We assume that some estimate $x^{(0)}$ of the solution is available. Literally hundreds of methods have been proposed for the solution of the nonlinear programming problem in the last decade[21]. The useful methods generally fall into two classes, transformation or linearization. This section contains a discussion of methods in each class along with pros and cons for each method.

### 3.1 Transformation methods

These methods transform the constrained

problem given in (3.1)-(3.3) into a sequence of unconstrained problems which are easier to solve. That is, given the functions $f(x)$, $g_j(x)$, and $h_j(x)$, we form the penalty function

$$P(x) = f(x) + \Omega(R,g(x),h(x)) \qquad (3.4)$$

where $\Omega$ is referred to as the penalty term and is a function of R, the penalty parameter, and the constraint values. There are many computer programs available which use the penalty function approach, including Fletcher's code in the HARWELL subroutine library[21].

The method of multipliers[22], which will now be discussed, addresses the major difficulty associated with all other penalty function methods, that of selecting and updating R. Here the parameter R is chosen and remains fixed throughout the entire optimization process. Furthermore, R becomes simply a scaling parameter which balances constraint violation with decreases in the objective. Other parameters are introduced and modified automatically from stage to stage under control of the algorithm, but the topology of the design space is much less drastically altered than before. Consider the function

$$P(x)=f(x)+R\sum_{j=1}^{J}\{\langle g_j(x)+\sigma_j\rangle^2-\sigma_j^2\}$$
$$+R\sum_{k=1}^{K}\{[h_k(x)+\tau_k]^2-\tau_k^2\}, \qquad (3.5)$$

where the bracket operator $\langle\cdot\rangle$ is defined by:

$$\langle\alpha\rangle = \begin{cases}\alpha & \text{if } \alpha \leq 0\\ 0 & \text{if } \alpha > 0\end{cases} \qquad (3.6)$$

The multipliers $\sigma_j$ and $\tau_k$ are fixed throughout each unconstrained minimization, but changed at the end of each stage using the following updating rule:

$$\sigma_j^{(m+1)}=\langle g_j(x^{(m)})+\sigma_j^{(m)}\rangle, \qquad (3.7)$$

$$j=1,2,3,\ldots,J,$$

$$\tau_k^{(m+1)}=h_k(x^{(m)})+\tau_k^{(m)},$$

$$k=1,2,3,\ldots,K, \qquad (3.8)$$

where $x^{(m)}$ minimizes the mth stage penalty function. Because of the bracket operator, $\sigma$ has no positive elements, whereas the elements of $\tau$ may be of either sign. These parameters serve as a bias in the arguments of the penalty terms, which together with the updating rules tend to increase the penalties associated with violated constraints, thus forcing successive minimization vectors $x^{(m)}$ toward feasibility. Quite importantly, the method leaves the curvature of the contours of the penalty function unchanged from stage to stage when the constraints are linear. Furthermore, when the constraints are nonlinear, there exists a second-order influence on the curvature of the contours of the penalty resulting from changes in $\sigma$ and $\tau$ from stage to stage. This approach has been implemented in the computer program BIAS[23], which was developed by Root and Ragsdell in the Design Group of the School of Mechanical Engineering at Purdue.

## 3.2 Linearization Approach- the Generalized Reduced Gradient Method

The reduced gradient method was originally given by Wolfe for a nonlinear objective function with linear constraints[24,25]. A generalization of Wolfe's method to accommodate nonlinearities in both the objective function and constraints was first accomplished by Abadie[26]. Concurrently to both Wolfe and Abadie, Wilde and Beighter developed their differential algorithm based on the constrained derivative[27]. The constrained derivative and the reduced gradient employ much the same theoretical basis, but for purposes of this discussion the method shall be known as the Reduced Gradient Method. The constrained nonlinear programming problem of (3.1)-(3.3) can be restated in the following form:

$$\text{Minimize: } f(x),\ x=[x_1,x_2,x_3,\ldots,x_N]^T \in R^N \qquad (3.9)$$

$$\text{Subject to: } h_\ell(x)\equiv 0 \quad \ell=1,2,3,\ldots,L \qquad (3.10)$$

$$A\leq x\leq B, \qquad (3.11)$$

where A and B are lower and upper bounds on the design variables respectively. The inequality constraints have been included as equality constraints through the following transformation:

$$h_j(x)=g_j(x)-S_j\equiv 0, \qquad (3.12)$$

$$0\leq S_j\leq\infty \quad j=1,2,3,\ldots,J. \qquad (3.13)$$

The variables $S_j$ are nonnegative slack variables, which must be included in the design variable set, so that N represents the number of slacks plus the original number of design variables. The design variables are divided into two classes, called state and decision variables, or

$$x=[z,y]^T, \qquad (3.14)$$

where z is the vector of decisions and y contains the states. We divide x such that there are exactly the same number of states as constraints. The decisions are completely free, whereas the states are slaves to be used to satisfy the constraints. Let us examine the first variation of the functions in (3.9) and (3.10):

$$df=\nabla_z f(x)^T dz+\nabla_y f(x)^T dy \qquad (3.15)$$

$$dh=\nabla_z h(x)dz+\nabla_y h(x)dy\equiv 0, \qquad (3.16)$$

where

$$\nabla_z f(x)= \left[\frac{\partial f}{\partial z_1},\frac{\partial f}{\partial z_2},\frac{\partial f}{\partial z_3},\ldots,\frac{\partial f}{\partial z_Q}\right]^T \qquad (3.17)$$

$$\nabla_y f(x)= \left[\frac{\partial f}{\partial y_1},\frac{\partial f}{\partial y_2},\frac{\partial f}{\partial y_3},\ldots,\frac{\partial f}{\partial y_L}\right]^T \qquad (3.18)$$

$$Q = N - L \qquad (3.19)$$

$$\nabla_z h(x) = \begin{bmatrix} \frac{\partial h_1}{\partial z_1}\frac{\partial h_1}{\partial z_2}\cdots\frac{\partial h_1}{\partial z_Q} \\ \frac{\partial h_2}{\partial z_1}\frac{\partial h_2}{\partial z_1}\cdots\frac{\partial h_2}{\partial z_Q} \\ \cdot \\ \cdot \\ \cdot \\ \frac{\partial h_L}{\partial z_1}\frac{\partial h_L}{\partial z_2}\cdots\frac{\partial h_L}{\partial z_Q} \end{bmatrix} \text{(LXQ)}. \quad (3.20)$$

$$\nabla_y h(x) = \begin{bmatrix} \frac{\partial h_1}{\partial y_1}\frac{\partial h_1}{\partial y_2}\cdots\frac{\partial h_1}{\partial y_L} \\ \frac{\partial h_2}{\partial y_1}\frac{\partial h_2}{\partial y_2}\cdots\frac{\partial h_2}{\partial y_L} \\ \cdot \\ \cdot \\ \cdot \\ \frac{\partial h_L}{\partial y_1}\frac{\partial h_L}{\partial y_2}\cdots\frac{\partial h_L}{\partial y} \end{bmatrix} \text{(LXL)}. \quad (3.21)$$

Now solve (3.16) for dy:

$$dy = -[\nabla_y h(x)]^{-1}\nabla_z h(x)dz. \quad (3.22)$$

Substituting (3.22) into (3.15) and rearranging yields the following linear approximation to the reduced gradient:

$$\nabla_r f(x)^T = \nabla_z f(x)^T - \nabla_y f(x)^T [\nabla_y h(x)]^{-1} \quad (3.23)$$

$$\nabla_z g(x).$$

The reduced gradient defines the rate of change of the objective function with respect to the decision variables, with the state variables adjusted to maintain feasibility. Expression (3.23) gives the changes necessary in the states for a given change in the decisions for linear constraints. Geometrically, the reduced gradient can be described as a projection of the original N-dimensional gradient onto the (N-L)-dimensional feasible region described by the decision variables. A necessary condition for the existence of a minimum of an unconstrained nonlinear function is that the elements of the gradient vanish. Similarly, a minimum of the constrained nonlinear function occurs when the appropriate elements of the reduced gradient vanish. A computer code, OPT, utilizing the Generalized Reduced Gradient Method has been developed by Gabriele and Ragsdell(28) in the Design Group of the School of Mechanical Engineering at Purdue.

### 3.3 Scaling

Very often in practice we encounter nonlinear programming problems which are poorly scaled. This may occur for a variety of reasons, but most often due to numerical incompatibility of units employed. That is, one design variable may be in miles while another is in inches, or a constraint may measure in pounds per square inch while others are expressed in feet per second, acres, or feet. When the problem is poorly scaled we have difficulty comparing violations in the various constraints, and relating these constraint violations to changes in the objective value. Dr. Ronald R. Root has developed a scaling algorithm, as a part of his doctoral work[29] in the Design Group of the School of Mechanical Engineering at Purdue University. The goal of the method is to automatically scale or condition any nonlinear programming problem so as to increase the probability of success of modern NLP methods. The problem is transformed by definition of scaling parameters:

$$g_j'(x) = \alpha_j g_j(x) \quad (3.24)$$

$$h_k'(x) = \beta_k h_k(x) \quad (3.25)$$

and

$$x_i' = \eta_i x_i. \quad (3.26)$$

We define a matrix J which contains the constraint gradients as rows, and preset $\alpha_j$ and $\beta_k$ so that all constraint values at the starting point, $x^{(0)}$, are of order 10. We detect a poorly scaled variable or constraint by noticing rows and/or columns whose nonzero elements are all significantly greater in modulus than other elements in J. Once the poorly scaled variables and constraints are detected, we define $\alpha_j$, $\beta_k$, and $\eta_i$ so as to produce roughly equal gradient sensitivities. The details are given by Root[30]. This scaling algorithm has proven to be very useful, if not indispensable in obtaining the numerical results reported in the next section.

The general utility of these and other algorithms for engineering design applications has recently been demonstrated by Sandgren[31], and a portion of his results is given in Figure 7. The curve marked "Enhanced BIAS" denotes the performance of the Method of Multipliers with Root's scaling algorithm, and OPT and BIAS (without scaling) are algorithms 11 and 1 respectively in the figure. Quite abviously OPT and BIAS are among the very best NLP algorithms available today.

## 4. NUMERICAL RESULTS

Using OPT and BIAS and the previously described optimal design formulation, we have sought the plant design which minimizes the normalized operating cost of generation of 600MW for ten hours each weekday. We have employed the Media, Illinois Galesville aquifer as the storage reservoir. Contour maps and material properties for this aquifer and other problem parameters, are given by Sharma[14], Katz[11] and Ahluwalia[32]. The subsystem 1 problem was solved for a number of combinations of $P_{ti}$ and $\dot{m}'$ using BIAS with automatic scaling. Recall that BIAS does not require a feasible starting point.

Contours of constant minimized operating cost for subsystem 1 are shown in Figure 8. A very significant cost variation is evident. The steeply rising cost at high pressure reflects the presence of a constraint, built into the aquifer mathematical model rather than appearing directly in the optimization problem constraint definitions. This constraint insists that the mean weekly pressure in the aquifer should equal its natural "discovery" pressure (840 psia in this example) in order to maintain a constant mean air storage volume. Figure 8, indicates that small $\dot{m}'$ values (i.e., low air flow rates) are favored. This is due primarily to the higher cost of the air storage reservoir as the quantity of air stored is increased.

The optimum subsystem 1 designs corresponding to points in Figure 8 were also found to vary widely. Of particular interest is the number of wells required. It was found to vary from a low of 54 in the lower left (low cost) region to values in the 200-500 range in the upper right region. Finally, it is noted that the effects of the discrete variables (low pressure compressor compression ratio, wellbore diameter, and main pipe diameter) have been studied, for one set of coupling variables, and are reported by Ahrens[33]. The only significant variation is due to wellbore diameter, which causes the cost to increase for increasing diameter. For the present study, these discrete variables are held fixed at optimal or near optimal values. The subsystem 2 problem was solved using OPT. Contours of constant minimized operating cost for subsystem 2 are presented in Figure 9 for a range of $p_{ci}$ and $\dot{m}'$ values. The minimum cost contour (22 mills/kWh) corresponds approximately to designs having the minimum allowed (1500°F) turbine inlet temperatures, $T_3$ and $T_5$. These correspond to conventional designs proposed for CAES plants. The maximum cost contour (24.5 mills/kWh) shown is near to the constraint boundry representing the upper limit (2400°F) on turbine inlet temperatures. These are advanced designs requiring considerable cooling air. From the overall system viewpoint, the advantage of these turbines is that they reduce the amount of air which must be stored (proportional to $\dot{m}'$), thus reducing the reservoir cost. The results in Figure 9 are based on $r_p$=16. It was found that use of $r_p$=11 yielded similar, but slightly higher, cost results throughout the region explored. The optimum recuperator effectiveness, ε, was found to vary from 0.52 to 0.77 for the ranges of coupling variables yielding solutions. The most common value encountered was on the order of 0.7.

By the nature of the decomposition strategy employed in this study, the optimum CAES plant (that design which minimizes the power generation cost for the specified utility load cycle and aquifer site) may be easily found by superposing the results from Figures 8 and 9. The resulting minimized cost contours are shown in Figure 10. Interestingly, even though the individual subsystem contours are open, their sum exhibits an overall optimum which is within the coupling variable domain considered. Figure 10 demonstrates that the power generation (operating) cost of the optimum CAES plant is slightly under 37.75 mills/kWh, and that the optimum values for the coupling variables are, approximately, $p_{ci}$=625 psia and $\dot{m}'$= 8.5 lbm/kWh. Knowing the optimum coupling variables, one can readily obtain the optimum values of other design variables from the separate subsystem 1 and 2 optimization results. These, and some pertinent dependent variable values, are indicated in Table 1. The associated cost components for the optimal and an initial feasible design are listed in Table 2. It is of interest to note that the constraints active at the solution are the three associated with the requirements that (a) the well spacing should not exceed the maximum spacing consistent with efficient aquifer utilization (as dictated by unsteady flow considerations), (b) the wells should not penetrate the air bubble so as to allow water coming into the well during a discharge process, and (c) the weekly minimum aquifer pressure should not drop below that required to maintain flow into the turbines. The low pressure turbine inlet temperature ($T_5$) is at its upper bound (2400°F) at the solution. Finally, the charging time durations were found to take their maximum allowed value on weeknights, but not on the weekend.

## 5. DISCUSSION

The optimal design approach affords a significant opportunity for cost savings in the construction and operation of compressed air energy storage systems; as can be seen from the previously given results. On the other hand, the models necessary to adequately represent such a practical physical system can be quite complex. We have given what we feel to be the least complex system model, which will produce a meaningful optimal design. Even with our simplified approach the complete CAES system optimization (including subsystems 1 and 2) involves 20 design variables, 4 discrete design parameters, 8 linear constraints, 5 nonlinear constraints, upper and lower bounds on all design variables, and a nonlinear objective function. Furthermore, the model includes functions which require calculation of the modified Bessel functions of the first and second degree and first and second kind, and various spline approximations for empirical data.

We expected the full CAES problem (that is, including subsystems 1 and 2) to provide a significant challenge to modern nonlinear programming methods. We sought relief in decomposition theory, whereby the largest NLP contained 16 design variables, 12 constraints, variable bounds and a nonlinear objective. We did, of course, have to solve the resulting optimization problems for various values of the coupling variables. Our experiments with subsystem 1 and 2 support our original fears concerning the difficulty of the complete CAES problem. Furthermore, the subsystem optimization problems have value within themselves. That is, these subgroups results provide insights that would be difficult at best to gather in any other way. Finally, the decomposition strategy employed here allows an orderly modular approach of design to be employed. That is, we might envision a different storage system (such as a hard rock cavern) which would produce a different subsystem 1 model. We could perform the subsystem 1 optimizations and synthesize the overall system results just as before. That is, the subsystem 2 results would be unaffected.

The results presented in Figures 8, 9, and 10 demonstrate an interesting consequence of the decomposition strategy. Subsystem 2 results show a very simple dependence on the coupling variables which is intuitively satisfying. Subsystem 1 results also show a somewhat simple variation with changes in $p_{t1}$ and $\dot{m}'$. Interestingly, neither of the subsystems had an optimum inside the design space explored. However, once the two subsystem results were combined, a distinct minimum is found. Another benefit of decomposition in this particular problem is that for the purpose of plant site selection, only subsystem 1 results need be considered. When one of many available sites is to be selected, as is the case with a proposed CAES pilot plant in Indiana or Illinois, the geological and cost data for the various aquifers can be input to the procedure and the optimal designs of subsystem 1 at various sites can then be compared in making the final decision. However, since different sites might have different base electricity cost, etc., a consideration of the interactions of subsystem 1 and 2 with subsystem 3 may be important to the evaluation. An interesting aspect of the optimization of subsystem 1, showing the great value of optimal design, is as follows. The authors originally felt, based on engineering judgment, that the CAES plant for the site assumed in this study should be designed with $p_{t1} \cong 750$ psia and $\dot{m}' \cong 10.4$ lbm/kWh. In a preliminary paper on CAES system design (14), results for an intuitive subsystem 1 design and an optimized design were presented. The former had a capital cost of $101.6 million, an operating cost of 24.25 mills/kWh and 700 wells, while the latter had a $62 million capital cost, 19.36 mills/kWh operating cost and 402 wells. Finally, referring to information in Tables 1 and 2, it was found that the subsystem 1 design at system optimum have a capital cost of only $22.26 million, an operating cost of 12.51 mills/kWh and only needed 54 wells!

In conclusion, it can be stated that a computer-aided optimal design technique has been developed, and applied, for design of a complex power system with energy storage. The results presented demonstrate the great value of the optimization approach, in general, and of the decomposition method, in particular, for this type of system.

ACKNOWLEDGEMENTS

The authors with to thank the U.S. Department of Energy, Division of Energy Storage; The Argonne National Laboratory, Energy and Environmental Systems Division, The Purdue Research Foundation, and The School of Mechanical Engineering at Purdue for their support of this research. We are also indebted to C.S. Kim, Phyllis Fuja and Jon Davis for their assistance.

Table 1. Optimal CAES Plant Design

| | |
|---|---|
| Number of wells | 54 |
| Active well-field area (acres) | 276.1 |
| Air bubble thickness (ft.) | 69.75 |
| Average active formation thickness (ft.) | 45.45 |
| Wellbore diameter (in.) | 7.0 |
| Surface area to be purchased (acres) | 1973 |
| Main piping diameter (in.) | 48 |
| Total weekly storage time (hrs.) | 52.1 |
| Compressor power required (MW) | 371 |
| Compressor system discharge pressure (psia) | 969 |
| Low pressure compressor pressure ratio | 11.0 |
| Recuperator effectiveness | 0.715 |
| Low pressure turbine inlet temperature (°F) | 2400 |
| High pressure turbine inlet temperature (°F) | 1625 |
| Premium fuel heat rate (Btu/kWh) | 4230 |
| Inlet pressure to subsystem 2 (psia) | 625 |
| Specific turbine system air flow rate (lbm/kWh) | 8.5 |

Table 2: CAES Plant Costs

| Capital Items | Initial Feasible Design ($10⁶) | Optimal Design ($10⁶) |
|---|---|---|
| Land | 8.843 | 2.959 |
| Piping | 3.449 | 3.449 |
| Bubble Development | 6.818 | 1.407 |
| Well Construction | 73.379 | 5.637 |
| Low Pressure Compressor | 4.642 | 4.486 |
| Booster Compressor | 4.455 | 4.656 |
| Recuperator | 3.643 | 3.102 |
| Turbine System | 7.054 | 12.553 |
| Balance-of-Plant | 42.000 | 42.000 |
| Total Capital Cost | 154.283 | 80.249 |
| **Other** | | |
| Base Load Electricity (mill/KWH) | 11.450 | 9.662 |
| Premium Fuel (mill/KWH) | 9.715 | 10.723 |
| Subsystem 1 Operating Cost | 24.25 | 12.51 |
| Subsystem 2 Operating Cost | 21.99 | 23.12 |
| Total Power Generation Cost (mill/KWH) | 46.24 | 35.63 |

REFEPENCES

1. Z. S. Stys, Proc. of Workshop on CAES Systems, Airlie House, Virginia, 18-19 Dec., 1975, ERDA-76-124 (1976).

2. H. H. Chiu, L. W. Rodgers, Z. A. Saleem, R. K. Ahluwalia, G. T. Kartsounes, and F. W. Ahrens, AIAA 16th Aerospace Sciences Meeting, Huntsville, AL, 16-18 Jan. 1978, AIAA paper 78-281 (1979).

3. An Assessment of Energy Storage Systems Suitable for Use By Electric Utilities, EM-264, EPRI Project 225, Public Service Electric and Gas Company, NJ, ERDA E(11-1) -2501 final report (1975).

4. J. B. Bush, Jr., principal investigator, Economic and Technical Feasibility Study of Compressed Air Storage, ERDA 76-76, March (1976).

5. A. J. Giramonti, principal investigator, Preliminary Feasibility Evaluation of Compressed Air Storage Power Systems, ERDA report CONS/NSF/ 42-1, Dec. (1976).

6. K. G. Vosburgh, AIAA J. of Energy 2, 106 (1978).

7. C. S. Kim and G. T. Kartsounes, A Parametric Study of Turbine Systems for Compressed Air Energy Storage Plants, Final Report for FY 1977. Argonne National Laboratory report ANL/ES-64, April(1978).

8. C. S. Kim and G. T. Kartsounes, Proc. of Compressed Air Energy Storage Technology Symp. Pacific Grove, California, Rep. CONF-780599, Jan. 1979.

9. P. A. Berman, ASME paper 76-JPGC-GT-1 (1976).

10. D. K. Kreid and M. A. McKinnon, CAES Advanced Systems Analysis, final report for FY 1977, Battelle Pacific Northwest Laboratories, Washington, Oct. (1977).

11. D. L. Katz and E. R. Lady, Compressed Air Storage for Electric Power Generation. Ulrich's Books, Inc., Ann Arbor, Michigan (1976).

12. R. K. Ahluwalia, A. Sharma, and F. W. Ahrens, Proc. Compressed Air Energy Storage Technology Symposium, Pacific Grove, California, pp. 295-325, CONF-780599 (Jan. 1979).

13. W. R. Davison, and R. D. Lessard, Study of Selected Turbomachinery Components for Compressed Air Storage Systems, Prepared by United Technologies Research Center for Argonne National Laboratory, Report ANL/EES-TM-14 (Nov. 1977).

14. A. Sharma, H. H. Chiu, F. W. Ahrens, R. K. Ahluwalia and K. M. Ragsdell, "Design of Optimum Compressed Air Energy-Storage Systems", Energy 4, pp. 201-216, (1979).

15. F. W. Ahrens, A. Sharma and K. M. Ragsdell, "Computer Aided Optimal Design of Compressed Air Energy Storage Systems", ASME 5th Design Automation Conference, St. Louis, MO, Sept. 9-12, 1979, to appear ASME Journal of Mechanical Design.

16. C. S. Kim, and G. T. Karsounes, A Parametric Study of Turbine Systems for Compressed Air Energy Storage Plants, Final Report for FY 1977 Argonne National Laboratory Report ANL/ES-64 (April 1978).

17. C. S. Kim, and G. T. Karsounes, Proc. of Compressed Air Energy Storage Technology Symposium, Pacific Grove, California, pp. 443-476, CONF-780599 (Jan. 1979).

18. G. T. Kartsounes, and C. S. Kim, "Evaluation of Turbomachinery for Compressed Air Energy Storage Plants", Proc. of the 1978 Mechanical and Magnetic Energy Storage Contractors' Review Meeting, Luray, Virginia, CONF-781046, pp. 417-425, (Oct. 1978).

19. G. B. Dantzig, Linear Programming and Extensions. Princeton University, New Jersey (1963).

20. P. E. Gill and W. Murray, Numerical Methods for Constrained Optimization. Academic Press, New York (1974).

21. R. Fletcher, In: Nonlinear Programming 2, p. 121. Academic Press, New York (1975).

22. S. B. Schuldt, G. A. Gabriele, R. R. Root, E. Sandgren, and K. M. Ragsdell, ASME J. Engng Industry 99 (Series B), 31 (1977).

23. R. R. Root and K. M. Ragsdell, BIAS: A Nonlinear Programming Code in Fortran-IV-Users Manual, Purdue Research Foundation, June (1976).

24. P. Wolfe, Nonlinear Programming, p.99. North Holland, Amsterdam (1967).

25. P. Wolfe, Recent Advances in Mathematical Programming, p. 76. McGraw-Hill, New York (1963).

26. J. Abadie and J. Carpentier, Optimization, p. 37. Academic Press, New York (1969).

27. D. J. Wilde and C. S. Beightler, Foundations of Optimization, Prentice-Hall, Englewood Cliffs, New Jersey (1967).

28. G. A. Gabriele and K. M. Ragsdell, OPT: A Nonlinear Programming Code in Fortran-IV-Users Manual, Purdue Research Foundation, June (1967).

29. R. R. Root, An investigation of the method of multipliers. Ph.D. dissertation, School of Mechanical Engineering, Purdue University, West Lafayette, Indiana, Sept. 1977.

30. R. R. Root and K. M. Ragsdell, "Computational Enhancements to the Method of Multipliers", 1979 ASME Design Automation Conference, paper no. 79-DET-77, St. Louis, MO., Sept. 1979, to appear in ASME Journal of Mechanical Design.

31. E. Sandgren and K. M. Ragsdell, "The Utility of Nonlinear Programming Algorithms: A Comparative Study, Part 1 & II, ASME 5th Design Automation Conference, St. Louis, MO, Sept. 9-12, 1979, to appear ASME Journal of Mechanical Design.

32. R. K. Ahluwalia, A. Sharma, and F. W. Ahrens, Proc. Compressed Air Energy Storage Technology Symp., Pacific Grove, California, Rep. CONF-780599, Jan. 1979.

33. F. W. Ahrens, "The Design Optimization of Aquifer Reservoir-Based Compressed Air Energy Storage Systems", Proc. of the 1978 Mechanical and Magnetic Energy Storage Contractors' Review Meeting, Luray, Virginia, CONF-781046, pp. 404-415, (Oct. 1978).

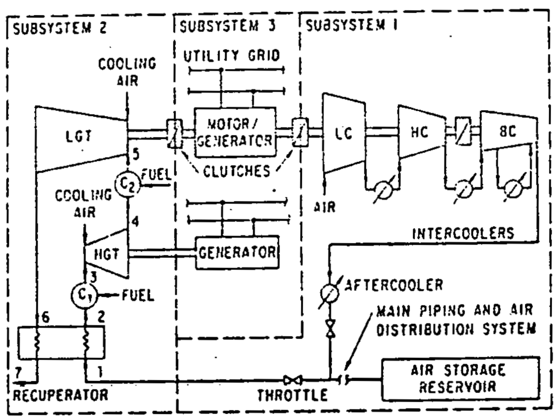


Figure 1: CAES Power Plant

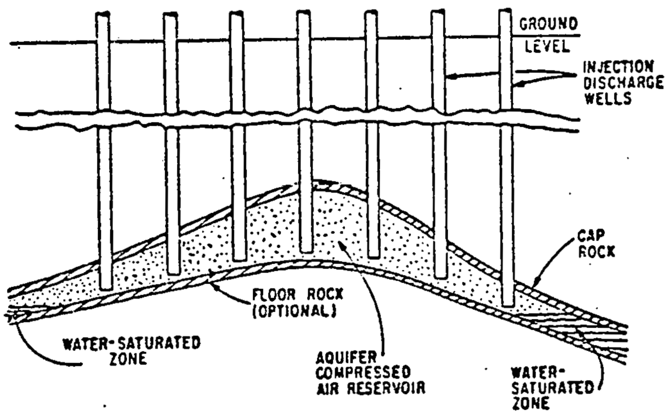


Figure 2: Edge Water Aquifer

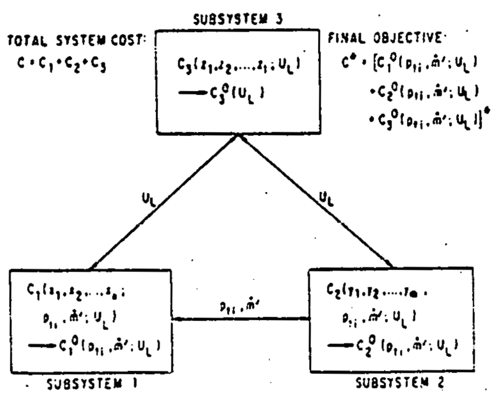


Figure 3: CAES Decomposition Strategy

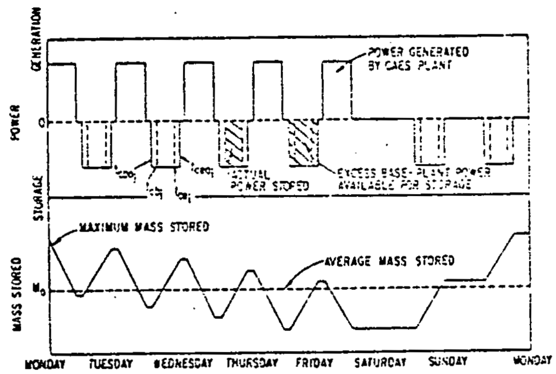


Figure 4: Utility Load Cycle ($U_L$)

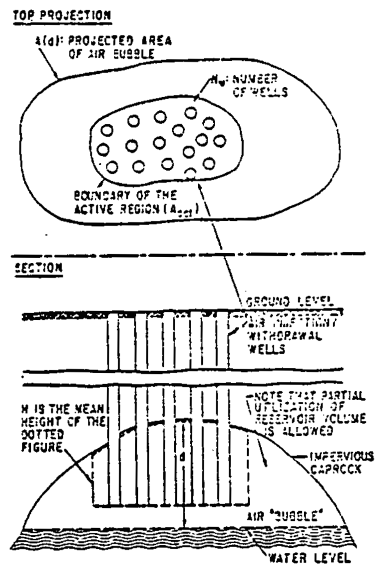


Figure 5: Aquifer Reservoir Geometry

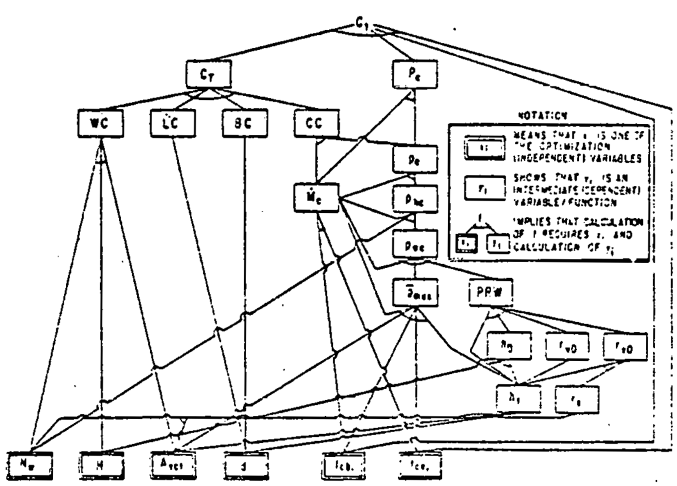


Figure 6: Calculation Flow for Subsystem 1

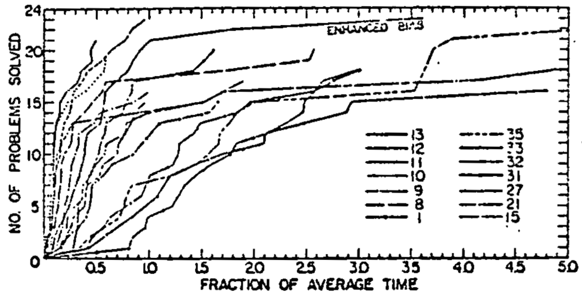


Figure 7: Utility of NLP Methods

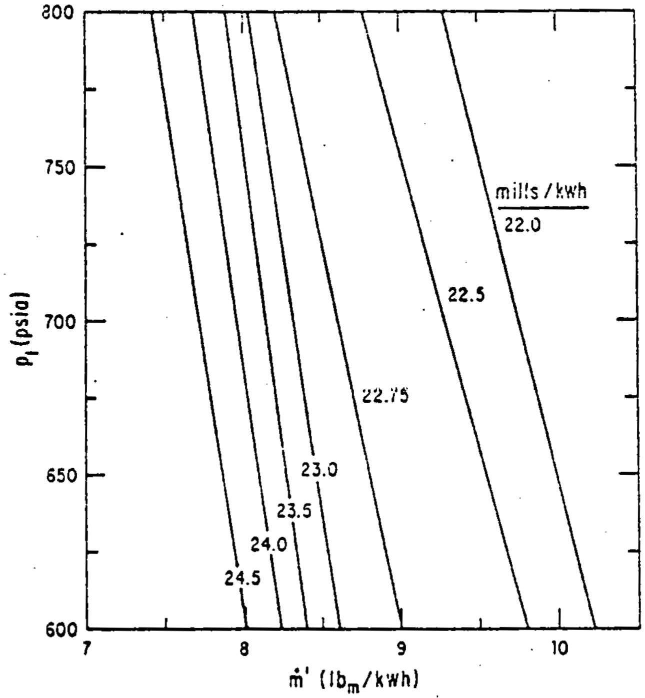


Figure 9: Subsystem 2 Optimization Results

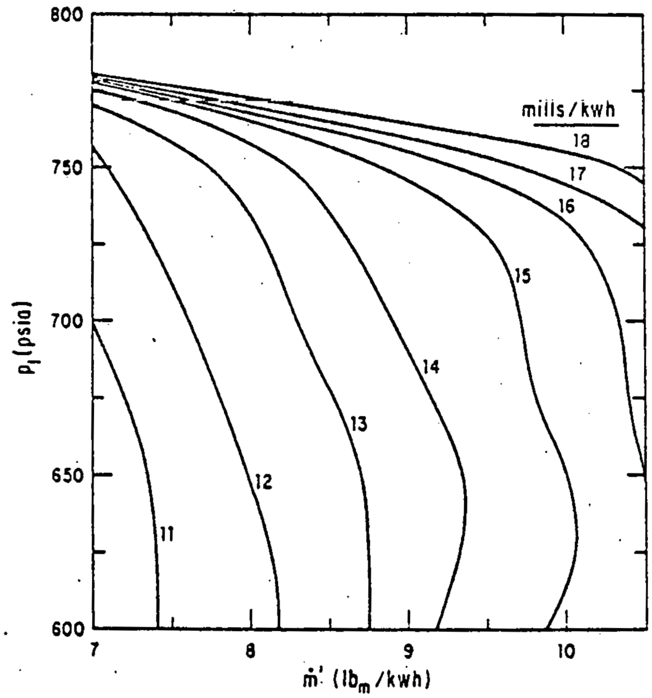


Figure 8: Subsystem 1 Optimization Results

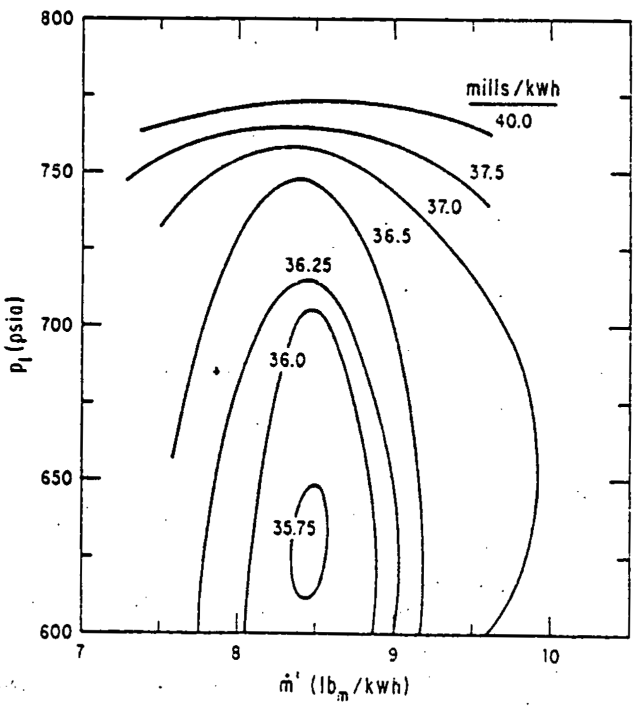


Figure 10: CAES Plant Optimization Results